Journal of Thermal Analysis and Calorimetry, Vol. 69 (2002) 997–1004

MOLECULAR DYNAMICS STUDY ON LATTICE DEFECTS AND HEAT CAPACITY OF $LiCr_{1/6}Mn_{11/6}O_{4-\delta}$

M. Tachibana[1], *T. Tojo*[1], *H. Kawaji*[1], *T. Atake*[1*], *N. Morita*[2], *H. Ikuta*[2], *Y. Uchimoto*[2] *and M. Wakihara*[2]

[1]Materials and Structures Laboratory, Tokyo Institute of Technology, 4259 Nagatsuta-cho, Midori-ku, Yokohama, 226-8503 Japan
[2]Department of Applied Chemistry, Graduate School of Science and Engineering,Tokyo Institute of Technology, 2-12-1 Ookayama, Meguro-ku, Tokyo, 152-8552 Japan

Abstract

Heat capacity of spinel $LiCr_{1/6}Mn_{11/6}O_{4-\delta}$ (δ=0, 0.0184) was measured between 5 and 300 K. Both compounds showed no anomaly in the measured temperature range, especially around the room temperature where a structural phase transition is reported for the parent compound $LiMn_2O_4$. The non-stoichiometric compound $LiCr_{1/6}Mn_{11/6}O_{3.9816}$ has greater heat capacity than that of the stoichiometric $LiCr_{1/6}Mn_{11/6}O_4$. Molecular dynamics study on the vibrational property of $LiMn_2O_{4-\delta}$ revealed that the lattice defects in the non-stoichiometric compound increase the low frequency phonons compared with the stoichiometric compound. It should be related to the greater heat capacity of the non-stoichiometric compound $LiCr_{1/6}Mn_{11/6}O_{3.9816}$.

Keywords: heat capacity, lithium manganese oxides, molecular dynamics simulation, non-stoichiometry, spinel

Introduction

The spinel-type lithium manganese oxide $LiMn_2O_4$ and its related materials are promising candidates for application as cathode materials in rechargeable lithium-ion batteries [1]. One of the problems associated with $LiMn_2O_4$, however, is the rapid capacity fading during charge/discharge cycles, which should be at least partly due to the reversible cubic-orthorhombic transition close to room temperature [2, 3]. The transition has been attributed to a cooperative Jahn–Teller distortion on the Mn^{3+} sites [4], which can be suppressed by the substitution of a fraction of Mn^{3+} with other metals in the mixed-valence Mn^{3+}/Mn^{4+} spinel $LiMn_2O_4$ [5, 6]. In recent years, the substitution with various metals has been explored to improve the cycle performance, and the highest performance is achieved by Co or Cr substituted samples [7, 8]. Also, the electrochemical properties of non-stoichiometric samples have been investigated for

* Author for correspondence: E-mail:atake1@rlem.titech.ac.jp

1418–2874/2002/ $ 5.00

Akadémiai Kiadó, Budapest
Kluwer Academic Publishers, Dordrecht

$LiMn_2O_{4-\delta}$ [9, 11, 12] and $LiM_yMn_{2-y}O_{4-\delta}$ (*M*=Cr, Co, Ni and Mg) [11, 12], and good cycle performances have been obtained in some cases.

The chemical composition $LiM_yMn_{2-y}O_{4-\delta}$ is used in previous papers to describe the non-stoichiometric compound. However, this expression is nominal and is not directly concerned with the defect structure such as oxygen vacancy. Two types of defect model are considered at present. One is the oxygen deficient model, in which some of the 32*e* anion sites in the spinel structure are assumed to be vacant [13, 14]. The other is the metal excess model, in which excess metal ions (Li, M, or Mn) occupy the empty 16*c* sites in the spinel [10–12]. Many efforts have been devoted to elucidate the defect structure of the non-stoichiometric $LiM_yMn_{2-y}O_{4-\delta}$, but the details are still not clarified.

In the present study, thermodynamic and vibrational properties of the spinel samples $LiCr_{1/6}Mn_{11/6}O_{4-\delta}$ (δ=0, 0.0184) prepared by controlling oxygen partial pressure at 1023 K have been investigated by heat capacity measurement and molecular dynamics simulation. Heat capacity of $LiCr_{1/6}Mn_{11/6}O_{4-\delta}$ (δ=0, 0.0184) was measured between 5–300 K, and molecular dynamics (MD) simulation of the metal excess model was performed to examine the structural and vibrational properties of the non-stoichiometric composition.

Method

Sample preparation and heat capacity measurement

Samples of spinel $LiCr_{1/6}Mn_{11/6}O_{4-\delta}$ were synthesized using the same method as described previously [11], in which the metal excess model was supported for the non-stoichiometry. $LiCr_{1/6}Mn_{11/6}O_4$ was prepared by reacting a stoichiometric mixture of $LiCO_3$, $MnCO_3$, and Cr_2O_3 at 873 K for 6 h and then at 1023 K for 72 h. The non-stoichiometric $LiCr_{1/6}Mn_{11/6}O_{4-\delta}$ was obtained by heating the stoichiometric sample at 1023 K under reduced oxygen partial pressure of –2.4 in $\log(P_{O_2}/\text{atm})$ by mixing N_2-balanced O_2 gas with pure N_2, followed by quenching into ice water. The compounds were single-phase spinels as characterized by powder X-ray diffraction. The lattice constants were 8.2358 Å for the stoichiometric sample and 8.2470 Å for the non-stoichiometric sample. The oxygen deficiency δ of the non-stoichiometric sample was determined thermogravimetrically to be 0.0184 from the mass change of the spinel by controlling P_{O_2} separately.

A relaxation calorimeter (PPMS, Quantum Design) was used for the heat capacity measurement between 5 and 300 K. The amounts of the samples used were 1.89 mg ($1.05\cdot10^{-5}$ mol) for $LiCr_{1/6}Mn_{11/6}O_4$ and 4.85 mg ($2.69\cdot10^{-5}$ mol) for $LiCr_{1/6}Mn_{11/6}O_{3.986}$.

Molecular dynamics simulation

The MD simulations were performed on $LiMn_2O_{4-\delta}$ ($0\leq\delta\leq0.02344$) with a fully ionized model using the MXDORTO program [15]. Interatomic forces in the present calculation are represented by effective pair-potentials in the following form:

$$V_{ij}(r_{ij}) = -\frac{Z_i Z_j e^2}{r_{ij}} + A_{ij}\exp\left(-\frac{r_{ij}}{\rho_{ij}}\right) - \frac{C_{ij}}{r_{ij}^6} \quad (1)$$

where $Z_i e$ is the charge of the i-th ion, r_{ij} is interatomic distance, and A_{ij}, ρ_{ij} and C_{ij} are constants.

The pair-potential consists of the long-range Coulomb term and a short-range function in the Buckingham form to model overlap-repulsion and dispersion forces. The constants used in the present study are given in Table 1. These values were derived from previous works by Ammundsen *et al*. [16, 17], and the Mn–O potential parameters were modified by no more than 2% to improve the structural model.

Table 1 The constants in the interatomic potentials for $LiMn_2O_{4-\delta}$

i–j	A_{ij}/eV	ρ_{ij}/Å	C_{ij}/eV Å^{-6}
Mn^{4+}–O^{2-}	1317.0	0.3163	0
Mn^{3+}–O^{2-}	1267.5	0.3214	0
[a]Li^{+}–O^{2-}	426.48	0.3000	0
[a]O^{2-}–O^{2-}	22764.3	0.1490	43.0

[a] From [16]

Table 2 Number of ions in the basic MD cell

$LiMn_2O_{4-\delta}$	Mn^{4+}	Mn^{3+}	Li^{+}	O^{2-}	Total
δ=0	512	512	512	2048	3584
δ=0.007797	505	521	513	2048	3587
δ=0.01556	498	530	514	2048	3590
δ=0.02344	491	539	515	2048	3593

During the simulation, temperature and pressure were controlled by means of the scaling of ion velocities and MD cell length, respectively. The calculations were run at 300 K and 0.1 MPa, using a time step of 2 fs and for a period of 100 ps after an initial equilibration of 10 ps. The velocity of ions was recorded every other step. The calculations were performed with a simulation box comprising 3584 ions (i.e. 4×4×4 spinel unit cells) in the case of $LiMn_2O_4$. Homogeneous distributions of Mn^{3+} and Mn^{4+} were assumed for $LiMn_2O_{4-\delta}$ containing manganese in a mixed oxidation state. For the $LiMn_2O_4$ (δ=0) structure, Mn^{3+} and Mn^{+} were distributed at random but homogeneously in the unit cell. For $LiMn_2O_{4-\delta}$, excess Mn^{3+} and Li^{+} ions were inserted at the 16*c* octahedral sites, while randomly replacing a number of Mn^{4+} with Mn^{3+} to keep the system electrically neutral. The numbers of ions in the basic simulation box for each simulation are given in Table 2. Simulations of different defect configurations within a simulation box were performed at least three times to confirm that the configuration of the defects has no effect on the results.

The phonon DOS $Z(\nu)$, where ν is frequency, was obtained from the Fourier transformation of the velocity autocorrelation:

$$Z(\nu) \propto \int_0^\infty \frac{<V(0)V(t)>}{<V(0)^2>} \cos(2\pi\nu t) \mathrm{d}t \tag{2}$$

where V(t) is the velocity of the ion at the time t. $Z(\nu)$ is normalized according to

$$\int_0^\infty Z(\nu)\mathrm{d}\nu = 3N_\mathrm{A} \tag{3}$$

where N_A is the Avogadro's number.

The heat capacity C_v was calculated from the DOS in a harmonic approximation:

$$C_\mathrm{v} = \frac{1}{k_\mathrm{B}} \int_0^\infty \left(\frac{h\nu}{\exp(h\nu/k_\mathrm{B}T) - 1} \right)^2 \frac{\exp(h\nu/k_\mathrm{B}T)}{T^2} Z(\nu)\mathrm{d}\nu \tag{4}$$

where k_B is the Boltzmann's constant and h is the Planck's constant.

Results and discussion

The heat capacity of $LiCr_{1/6}Mn_{11/6}O_{4-\delta}$ (δ=0, 0.0184) was measured between 5 and 300 K by the relaxation method. The results are shown in Fig. 1a. To compensate for the quantitative difference between the stoichiometric and non-stoichiometric compound, namely the difference in the number of atoms which compose one mole in those chemical formula, the results are plotted as the normalized heat capacity $C_\mathrm{p}^* = 7C_\mathrm{p}/(7-\delta)$ for comparison. No heat capacity anomaly was observed in both samples, suggesting, as in earlier studies [5, 6], that the cooperative Jahn–Teller transition was suppressed by the Cr substitution. For clarity, the heat capacity difference (ΔC_p^*) was derived from subtracting the normalized heat capacity of $LiCr_{1/6}Mn_{11/6}O_4$ from that of $LiCr_{1/6}Mn_{11/6}O_{3.9816}$ and is shown in Fig. 1b. The non-stoichiometric sample has greater heat capacity in all the temperature range, and the heat capacity difference increases with increasing temperature, while shallow minima are found at 70, 105, and 200 K. Such excess heat capacity should be attributed to the lattice defects due to the non-stoichiometry.

Molecular dynamics simulations of the stoichiometric $LiMn_2O_4$ and of the non-stoichiometric $(Li)_{8a}[Li_{\delta/(4-\delta)}Mn_{2\delta/(4-\delta)}]_{16c}[Mn_2]_{16d}[O_4]_{32e}$, in which excess metals occupy the vacant 16*c* sites in the spinel, were performed to investigate the microscopic origin of the heat capacity difference. In this paper, the non-stoichiometric spinel is represented as $LiMn_2O_{4-\delta}$ for the convenience of expression. For simplicity, MD simulations were performed on cubic $LiMn_2O_{4-\delta}$ without Cr substitution, since the substitution has been shown to have no effect on the defect structure [11, 12]. First, the evolution of the lattice constant and mass-density as a function of δ was calculated. The results are compared with the experimental values [10] as shown in

Fig. 2a for the lattice constant *a* and in Fig. 2b for the mass-density *d*. In these figures, the simulations show increase in the lattice constant and mass-density with increasing δ, which is in good agreement with the experiment.

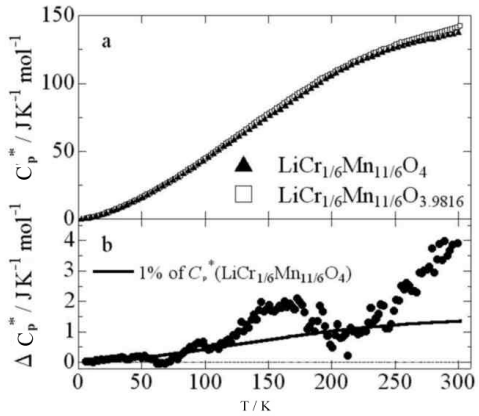

Fig. 1 a – Heat capacity of $LiCr_{1/6}Mn_{11/6}O_{4-\delta}$ (δ=0, 0.0184). The asterisk denotes the normalization $C_p^*=7C_p/(7-\delta)$ for quantitative comparison between the molar heat capacities of the compounds in which the number of constituent atom is different.
b – Heat capacity difference derived from subtracting the normalized heat capacity of $LiCr_{1/6}Mn_{11/6}O_4$ from that of $LiCr_{1/6}Mn_{11/6}O_{3.9816}$. The solid line represents the 1% of heat capacity of $LiCr_{1/6}Mn_{11/6}O_4$

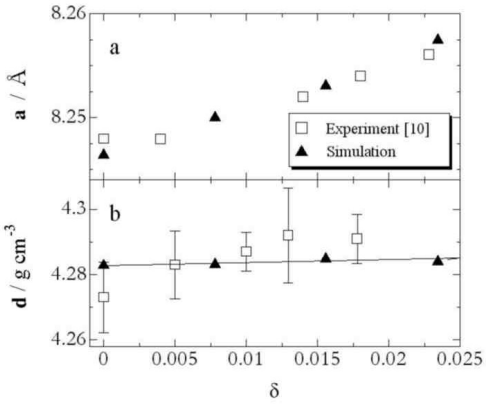

Fig. 2 Structural properties of $LiMn_2O_{4-\delta}$ plotted as a function of non-stoichiometry δ; a – for lattice parameter *a* and b – for mass-density *d*

The phonon DOS of $LiMn_2O_{4-\delta}$ with δ=0.02344 is compared with that of $LiMn_2O_4$ in Fig. 3. Only the low frequency range, which is relevant to the low-temperature heat capacity, is being compared in the main figure, and the DOS in the whole range are shown as the inset. The calculated phonon DOS exhibit peaks at

3.5, 5.2, 6.2 and 8 THz in the low frequency range. At lower frequencies below 7 THz, the DOS of $LiMn_2O_{4-\delta}$ is greater than that of $LiMn_2O_4$.

The calculated phonon DOS were used to derive the heat capacity C_v. The heat capacity difference $\Delta C_v^*=C_v^*(LiMn_2O_{4-\delta}) - C_v^*(LiMn_2O_4)$ with the normalization $C_v^*=7C_v/(7-\delta)$ is shown in Fig. 4. The correction of C_p-C_v was estimated to be negligibly small (<0.2%) in the temperature region under consideration. The non-stoichiometric composition shows a greater heat capacity than that of stoichiometric $LiMn_2O_4$, which corresponds to the greater phonon DOS of the former below 7 THz.

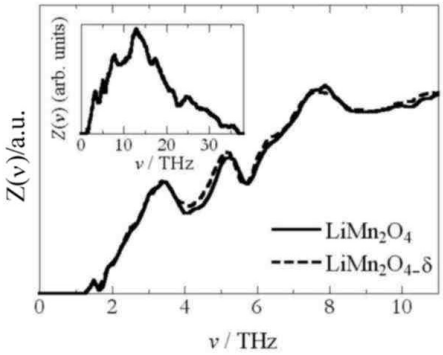

Fig. 3 The phonon DOS in the low frequency range calculated for $LiMn_2O_4$ and $LiMn_2O_{4-\delta}$ (δ=0.02344). Inset shows the DOS in the whole range

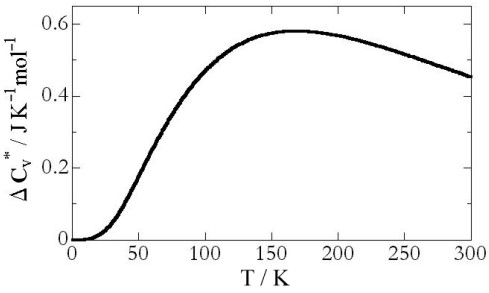

Fig. 4 Calculated heat capacity difference between $LiMn_2O_{4-\delta}$(δ=0.02344) and $LiMn_2O_4$ ($\Delta C_v^*=C_v^*(LiMn_2O_{3.97656})-C_v^*(LiMn_2O_4)$). The asterisk denotes the normalization $C_v^*=7C_v/(7-\delta)$

The phonon DOS in Fig. 4 were calculated from the sum total of the concentration weighted partial DOS of the ions. The partial DOS of each ion in $LiMn_2O_4$ and $LiMn_2O_{4-\delta}$ are shown in Fig. 5. The partial DOS of Li^+ ion is concentrated around 8 THz, while those of Mn^{4+} and Mn^{3+} have several concentrated regions in the low frequency range. The partial DOS of O^{2-} appears mostly in the higher frequency range. To determine the effect of the greater metals/oxygen ratio in $LiMn_2O_{4-\delta}$ on its

greater heat capacity, the phonon DOS of $LiMn_2O_{4-\delta}$ was calculated with the ratio of 1:1:1:4 for Mn^{4+}:Mn^{3+}:Li^+:O^{2-}. The effect was thus determined to be 30-40% of the whole heat capacity difference in all the temperature range.

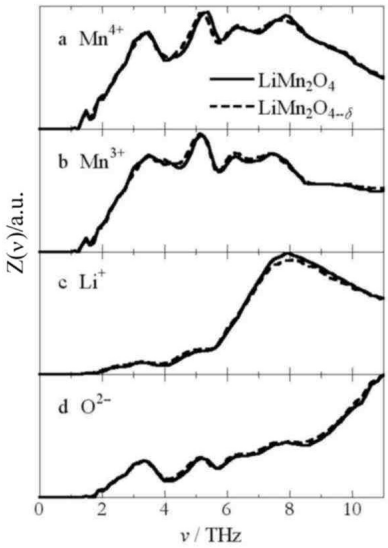

Fig. 5 Partial DOS in the low frequency range calculated for $LiMn_2O_4$ and $LiMn_2O_{4-\delta}$ (δ=0.02344). a – Mn^{4+}; b – Mn^{3+}; c – Li^+; d – O^{2-}

In Fig. 5, each ion shows peaks at 3.5, 6.2, and 5.2 THz, suggesting that cooperative vibrations of all ions are involved. Compared to other ions, these peaks are less pronounced in Li^+. Partial DOS of each ion in the low-frequency range is slightly greater in $LiMn_2O_{4-\delta}$ than in $LiMn_2O_4$, except for around 8 THz in Li^+ and Mn^{4+}. These increases indicate that a number of low frequency phonons are induced by the defect, which contribute to the greater heat capacity of the non-stoichiometric composition.

Conclusions

The low temperature heat capacity of the spinel $LiCr_{1/6}Mn_{11/6}O_{4-\delta}$ (δ=0, 0.0184) was measured between 5 and 300 K, and molecular dynamics simulation of $LiMn_2O_{4-\delta}$ with interstitial metals at vacant 16*c* sites was performed. The simulation reproduced the structural properties of non-stoichiometric lithium manganese oxides, and the greater heat capacity of the non-stoichiometric sample compared to the stoichiometric sample should be attributed to the defect-induced low frequency phonons.

* * *

The present work has financially been supported by the Grant-in-Aid for Scientific Research on Priority Areas (B) No.740 from the Ministry of Education, Culture, Sports, Science and Technology of Japan.

References

1 T. Ohzuku, M. Kitagawa and T. Hirai, J. Electrochem. Soc., 137 (1990) 769.
2 K. Oikawa, T. Kamiyama, F. Izumi, B. C. Chakoumakos, H. Ikuta, M. Wakihara, J. Li and Y. Matsui, Solid State Ionics, 109 (1998) 35.
3 G. Rousse, C. Masquelier, J. Rodriguez-Carvajal and M. Hervieu, Electrochem. Solid-State Lett., 2 (1999) 6.
4 H. Yamaguchi, A. Yamada and H. Uwe, Phys. Rev. B, 58 (1998) 8.
5 D. Song, H. Ikuta, T. Uchida and M. Wakihara, Solid State Ionics, 117 (1999) 151.
6 D. Capsoni, M. Bini, G. Chiodelli, V. Massarotti, C. B. Azzoni, M. C. Mozzati and A. Comin, Phys. Chem. Chem. Phys., 3 (2001) 2162.
7 L. Guohua, H. Ikuta, T. Uchida and M. Wakihara, J. Electrochem. Soc., 143 (1996) 178.
8 A. D. Robertson, S. H. Lu and W. F. Howard, Jr., J. Electrochem. Soc., 144 (1997) 3505.
9 A. Yamada, K. Miura, K. Hinokuma and M. Tanaka, J. Electrochem. Soc., 142 (1995) 2149.
10 M. Hosoya, H. Ikuta, T. Uchida and M. Wakihara, J. Electrochem. Soc., 144 (1997) L52.
11 M. Hosoya, H. Ikuta and M. Wakihara, Solid State Ionics, 111 (1998) 153.
12 N. Hayashi, H. Ikuta and M. Wakihara, J. Electrochem. Soc., 146 (1999) 1351.
13 J. Sugiyama, T. Atsumi, T. Hioki, S. Noda and N. Kamegashira, J. Power Sources, 68 (1997) 641.
14 R. Kanno, M. Yonemura, T. Kohigashi, Y. Kawamoto, M. Tabuchi and T. Kamiyama, J. Power Sources, 97-98 (2001) 423.
15 Japan Chemistry Program Exchange No. 029.
16 B. Ammundsen, J. Rozière and M. S. Islam, J. Phys. Chem. B, 101 (1997) 8156.
17 B. Ammundsen, G. R. Burns, M. S. Islam, H. Kanoh and J. Rozière, J. Phys. Chem. B, 103 (1999) 5175.